Forensic Science International: Reports 8 (2023) 100331

Contents lists available at ScienceDirect

Forensic Science International: Reports

journal homepage: www.sciencedirect.com/journal/forensic-science-international-reports

A geometric morphometric assessment of the hard tissue external auditory meatus and soft tissue ear of South Africans

Meg-Kyla Erasmus *, Ericka Noelle L'Abbé, Alison Fany Ridel

Forensic Anthropology Research Centre, Department of Anatomy, Faculty of Health Sciences, University of Pretoria, 9 Bophelo Road, Prinshof, Pretoria 0184, South Africa

ARTICLE INFO

Keywords:
Forensic anthropology
Facial approximation
External ear shape variation
Cone-beam computed tomography
Geometric morphometric methods
Anatomical and sliding landmarks

ABSTRACT

Research on how to reliably reconstruct the shape of the ear for facial approximations is limited, especially in countries such as South Africa where standard ear casts are still used in manual methods. To improve objectivity, computer aided methods are being developed for facial approximations – which require extensive population specific datasets for facial feature morphology. This study aims to assess variations in the shape of the ear and the underlying external auditory meatus (EAM) through the analysis of cone-beam computed tomography (CBCT) scans of 40 black South Africans (males n = 17; females n = 23) and 76 white South Africans (males n = 29; females n = 47) between the ages of 18 and 90 years. Shape data was collected by placing 19 capulometric landmarks on the 3D reconstructions of the ear and 46 sliding craniometric landmarks along the EAM. Geometric morphometric analysis revealed highly significant variation in ear shape between groups for population affinity (p-value = 0.001), while sex and age were only significant between the white South Africans (p-value < 0.05). Only population affinity significantly influenced shape in the EAM (p-value = 0.001), and both the ear and EAM showed significant levels of symmetry (p-value = 0.007). While an ear will never be exactly recreated, basing facial estimates on the decedent's biological profile can lead towards the highest possible accuracies. For the ear shape specifically, sex and age will not be a priority when creating predictive models, but population affinity will greatly influence the output.

Introduction

Due to the complexity of the ear's shape, information on how to create reliable estimates of the ear in forensic and clinical approximations is scarce and often contradictory in their approaches. In 1955, Russian anthropologist Mikhail Gerasimov provided guidelines for approximating the ear from dry skulls, with additional suggestions and alterations made in the years following. However, subsequent studies have disproven the Gerasimov's guidelines [1], finding no statistical correlation between cranial features and the external soft tissues of the ear [2,3]. As all existing guidelines have been proven unreliable, current methods of approximating the ear are open to artistic interpretation or standard ear casts are applied, scaled, and angled according to other facial proportions such as the nose and mandibular angle [2,4].

As the field moves towards automated facial approximation methods, various automated data collection techniques and methodologies are also being developed [5,6]. By correlating selected cranial landmarks of the unknown skull to soft tissue structures, a facial estimate can be generated from a database of population affinity-, age-, and sex-specific individuals matching the unknown's biological profile [7]. Computerized software for approximating facial estimates aids in eliminating the subjectivity associated with manual sculpting and minimizes human error [5]. However, subjectivity remains present in the operator's placing of landmarks on 3D images, leading researchers to recommend an automated landmarking procedure [7–9].

The morphology of the facial skeleton has repeatedly been correlated with ecogeographic factors and adaptions to broad geographical areas [10,11], but significant differences in temporal bone morphology were only observed amongst modern human populations in extreme climates [12]. It is currently unknown how such variance translates into an ear's shape. However, the broad geographical variations of past populations are reflected in their modern descendent groups, resulting in the morphological variations observed between modern black and white South Africans [10,13]. Within forensic anthropology in South Africa, these morphological traits are translated into the socio-culturally accepted labelling system for the sake of clarity within the broader

* Correspondence to: 9 Bophelo Road, Prinshof, Pretoria 0184, South Africa.
E-mail address: meg-kyla.erasmus@up.ac.za (M.-K. Erasmus).

https://doi.org/10.1016/j.fsir.2023.100331
Received 20 February 2023; Received in revised form 2 August 2023; Accepted 4 August 2023
Available online 6 August 2023

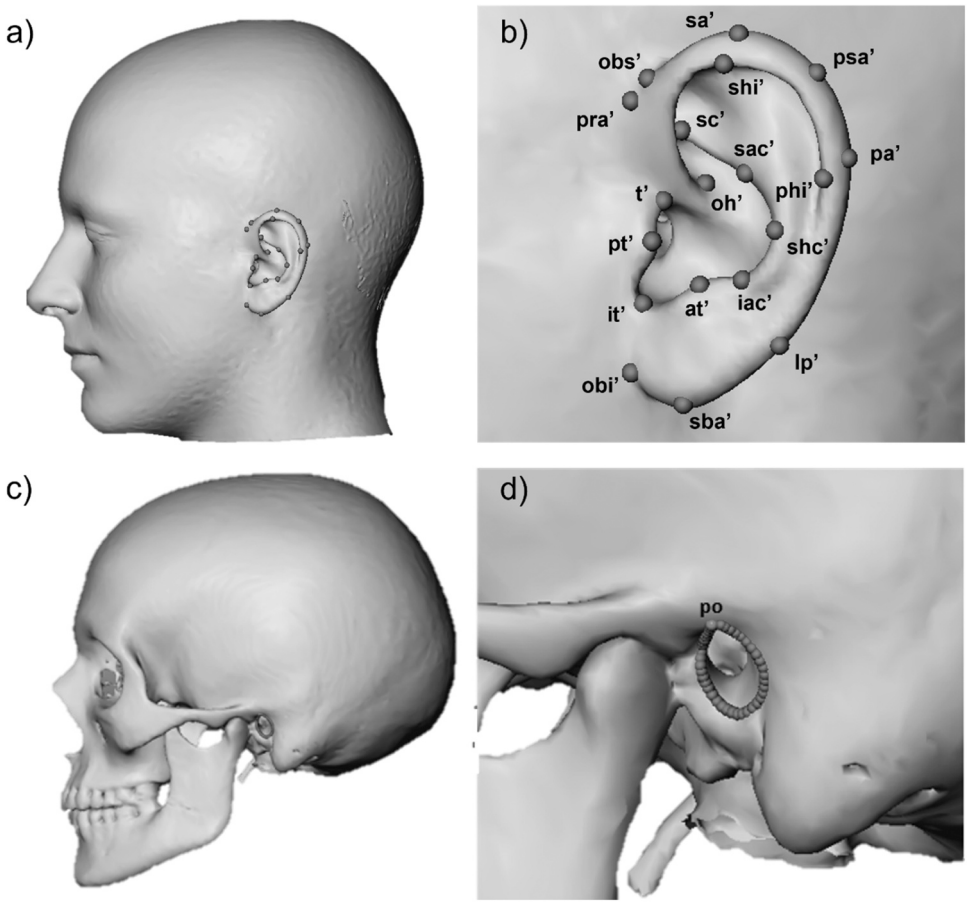

Fig. 1. Structures assessed in this study. a) Capulometric landmarks placed. b) Landmarks of the soft tissue ear. c) Craniometric landmarks placed. d) Sliding landmarks on the hard tissue external auditory meatus (EAM) starting at porion.

social context. Anthropologists subscribe to the same labelling system when compiling a biological profile (population affinity, sex, age, stature) to release to law enforcement or to compare to a list of missing persons.

Existing literature for variation in the ear focuses on assessing variation in ear size between populations, sex, and age groups with little to no regard to how any of these factors influence the shape of the outer ear [3,14–17]. Studies on shape variation focus on categorizing ears based on broad morphological categories (round, square, elongated), rather than complex statistical analyses [18]. Across the multiple population groups studied, males are consistently found to have larger ears than females for both height and width [3,14–17]. The external ear also undergoes significant changes with age, most notably in ear height elongating throughout an individual's lifetime, with the most significant lengthening occurring after 60 years [14,19,20]. Changes are attributed to ear tissue elasticity coupled with the effects of gravity [14–16]. The effects of age on ear size and shape studies are most noticeable when comparing studies on the same population groups but with different age categories. Guyomarc'h et al. [21] studied ear shapes on Computed Tomography (CT) scans of a French population using GMM, finding a significant variation in shape between sexes and age cohorts. However, the effect of supination in the use of traditional CT must be considered as it is known that supination causes capulometric landmarks to displace laterally on the x-axis, superiorly on the y-axis and posteriorly on the z-axis [22,23].

Cone-Beam Computed Tomography (CBCT) is an effective alternative to traditional CT for extracting hard and soft tissue surface meshes [21]. The upright scanning position also eliminates the supination effect, which is found in CT scans [23–25]. A Geometric Morphometric approach was used to extract and compare information encoded in the 3D surface representations of the shape of the ear and underlying bony structures. Geometric morphometric methods examines the mean shapes of structures, patterns of variation, group differences in shape and functional importance through the configurations formed by these anatomical landmarks and allow for the effective visual representation of statistical results as actual shapes [26–28].

This study aimed to assess variations in the shape of the soft tissue of the ear and the underlying external auditory meatus between populations, sex, and age cohorts in a South African sample.

Materials and methods

Materials

Cone Beam Computed Tomography scans of 116 individuals between the ages of 18 and 90 (mean age = 43 years) were collected from the University of Pretoria Oral and Dental Hospital and Groenkloof Life Hospital in Pretoria, South Africa. The sample comprised of 40 black South Africans (males n = 17; females n = 23) and 76 white South Africans (males n = 29; females n = 47). Exclusion criteria included: any trauma, pathology, surgical intervention, deformity, stretched tunnel piercings or if the patient's ears were compressed by scanning equipment. Ethical approval from the Research Ethics Committee of the Faculty of Health Sciences at the University of Pretoria was obtained under reference number 489/2020.

Table 1
Definitions of the anatomical and sliding landmarks used in this study.

No.	Abb	Landmark	Definition	Source
Soft tissue ear				
1	t'	Tragion	The notch above the tragus where the upper edge of the cartilage disappears into the skin of the face	[30]
2	pt'	Posterotragion	Most posterior point on the tragus	[30]
3	obi'	Otobasion inferius	Point of attachment of the ear lobe to the cheek	[21]
4	sba'	Subaurale	Most inferior point on the free margin of the auricle	[21]
5	lp'	Lobule posterior	Most posterior point of the lobule where it meets the helix	[32]
6	pa'	Postaurale	Most posterior point on the free margin of the auricle	[21]
7	phi'	Posterohelixa interna	Posterior most aspect of the inner helix margin	[30]
8	shi'	Superhelixa interna	Superior most aspect of the inner helix margin	[30]
9	sa'	Superaurale	Most superior point on the free margin of the auricle	[21]
10	obs'	Otobasion superius	Point of attachment of the helix in the temporal region	[21]
11	pra'	Preaurale	Most anterior point of the ear located just in front of the otobasion superius	[3]
12	sc'	Supraconchale	Most posterior point of the conchal rim where it cross under the helix	[30]
13	oh'	Origohelixa	Point of origin of the helix from the concha	[30]
14	at'	Antitragion	Apex of the antitragus	[30]
15	it'	Intertragion	Apex of the groove between the tragus and antitragus	[30]
16	iac'	Subanguili conchali	Inferior angle of the conchal rim	[30]
17	psa'	Posterosuperior aurale	Strongest helical curvature around the midpoint between superaurale and posteroaurale	new*
18	sac'	Supra-anguili conchali	Superior angle of the canchal rim	[30]
19	shc'	Strongest anti-helical curvature	The most posterior point of the conchal rim	[32]
Starting point for hard tissue sliding landmarks on the EAM				
1	po	Porion	Most superior point on the upper margin of the external auditory meatus	[30]

Methods

The CBCT images were imported into *MeVisLab 2.7.1* in DICOM format to generate 3D surface meshes using the Half Maximum Height quantitative iterative thresholding method [29]. For this study threshold values were between 250 and 500 for soft tissue surfaces and between 900 and 1 500 for hard tissue surfaces.

A combination of craniometric (hard tissue) and capulometric (soft tissue) landmarks were used in this study to assess shape variation in both the ear and underlying external auditory meatus (EAM) [30], whereas the use of sliding landmarks allow for clear visualization of curved structures to provide a more accurate assessment of shape. The use of standard biological landmarks ensures that each point identified is in the same location on all other surfaces in the sample and allows for homology and comparability between studies [28,30]. Nineteen capulometric landmarks on the soft tissue of the ear and 46 sliding landmarks surrounding the EAM were used to assess shape (Fig. 1, Table 1). For accurate analysis, each curve is required to have the exact same number of landmarks, and all curves must start in the same place. The standard landmark porion was selected as the starting landmark for each EAM. To increase objectivity of the landmark placements, the automated landmarking procedure published by Ridel and colleagues [31] was followed for anatomical shape extraction. This method involves the generation of a template from the superimposed segmentations of all individuals of the sample, where each point on the template corresponds to the same point on each individual surface. Placing a landmark on the template will allow the observer to automatically project the landmarks onto every individual in the sample.

Table 2
Average dispersion error for combined landmark configurations (in mm).

	Intra-OE		Inter-OE	
	Mean	**Sd**	**Mean**	**Sd**
Left ear	0.980	0.381	1.284	0.741
Right ear	0.758	0.290	1.689	0.802
Left EAM	0.849	0.049	0.357	0.196
Right EAM	0.537	0.043	0.538	0.084

EAM = external auditory meatus

Statistical analyses

Landmarks were tested for reproducibility using dispersion error to measure the average distance between the same landmark placed by different observers. For Intra-Observer Error (INTRA-OE), landmarks were placed on the template by the same observer two weeks apart and projected onto ten randomly selected scans in the sample. To assess reproducibility for Inter-Observer Error (INTER-OE), landmarks were placed on the template by two different observers, two weeks apart, and the results compared.

Geometric morphometric methods were applied on all four structures to quantify and visualize variation in shape, as well as assess how shape is influenced by population affinity, sex, and age of the individual. A General Procrustes Analysis (GPA) was performed on the hard and soft tissue Cartesian coordinates to obtain the mean shape coordinates [27, 33,34]. Principal Component Analysis (PCA) was used to create new independent Principal Component (PC) scores based on the outputs of the GPA. Principal Component scores represent the maximum variation of the original variables by identifying linear combinations to reduce the dimensionality of the data [27]. Multivariate normality testing through the interpretation of Q-Q plots was performed on the PC scores resulting from the PCA [35,36].

Asymmetry was assessed between the left and right ears and left and right EAM using the matching symmetry method to identify a significant variation in shape between the left and right sides of an individual [37]. Significance of population affinity, sexual dimorphism, and age effects were assessed through a MANOVA (using the R-package *geomorph* [38]), 50–50 MANOVA (applied using the R-package *ffmanova* [39,40]), and permutation testing (applied using the R-package *Morpho* [36]). To identify any population-specific differences, the influence of sex and age were performed on the entire sample, as well as on each population group separately.

As GMM removes scale as a factor, the effects of size in terms of allometry was assessed. Allometry assesses the influence size has on shape and is considered the most dominant factor of shape and form within a group in many data sets [41]. Allometry was assessed using linear models (hard and soft tissue shape versus the variables sex and centroid size) calculated using the PCs from the initial analysis. The significance of each variable was tested using Pillai trace using MANOVA and the non-parametric test 50/50 MANOVA. As size is largely influenced by sex and for ears especially by age, allometry was assessed on each subset separately.

A standard Discriminant Function Analysis (DFA) was applied using the R-package *Morpho* to assess the accuracies of classifying population affinity, sex, and age by ear or EAM shape through leave-one-out cross-validation [36].

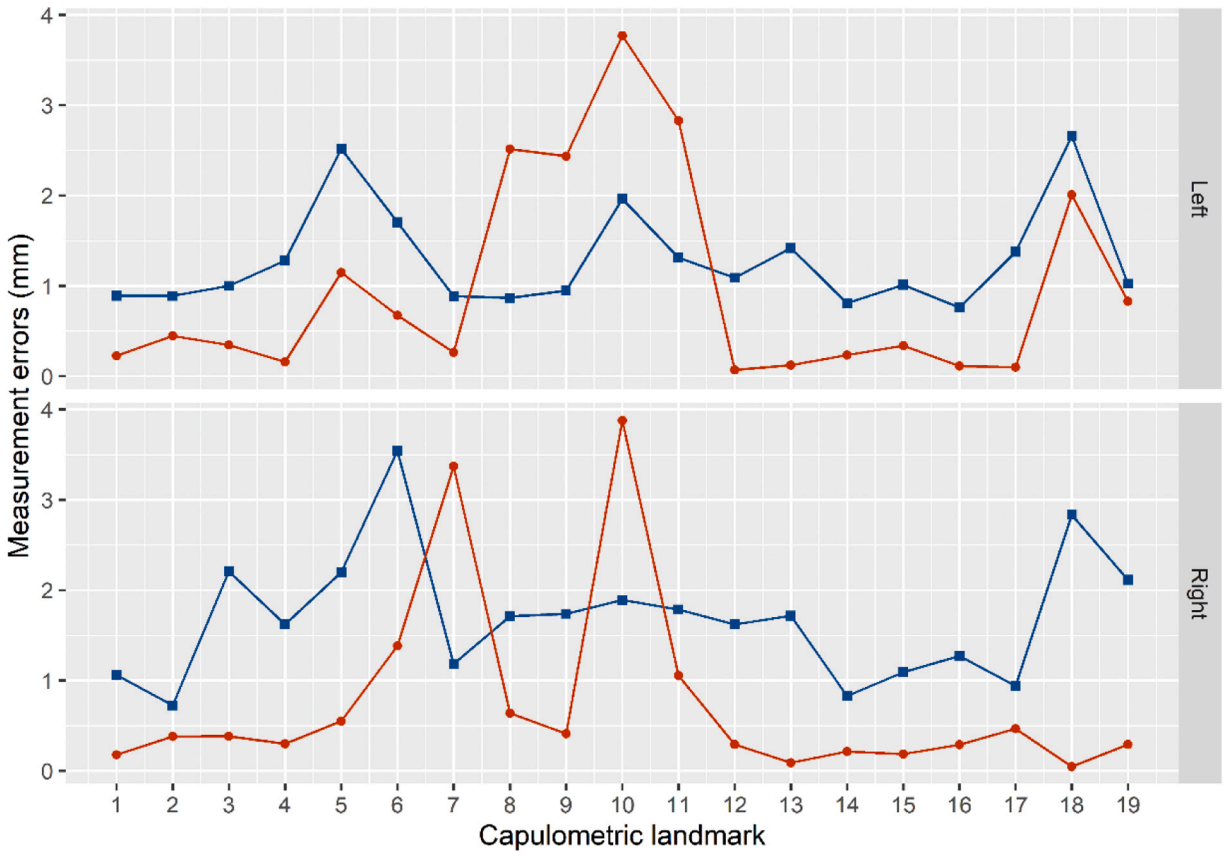

Fig. 2. Average dispersion for capulometric landmark placements (soft tissue ear). Red circle represents INTRA-OE. Blue square represents INTER-OE.

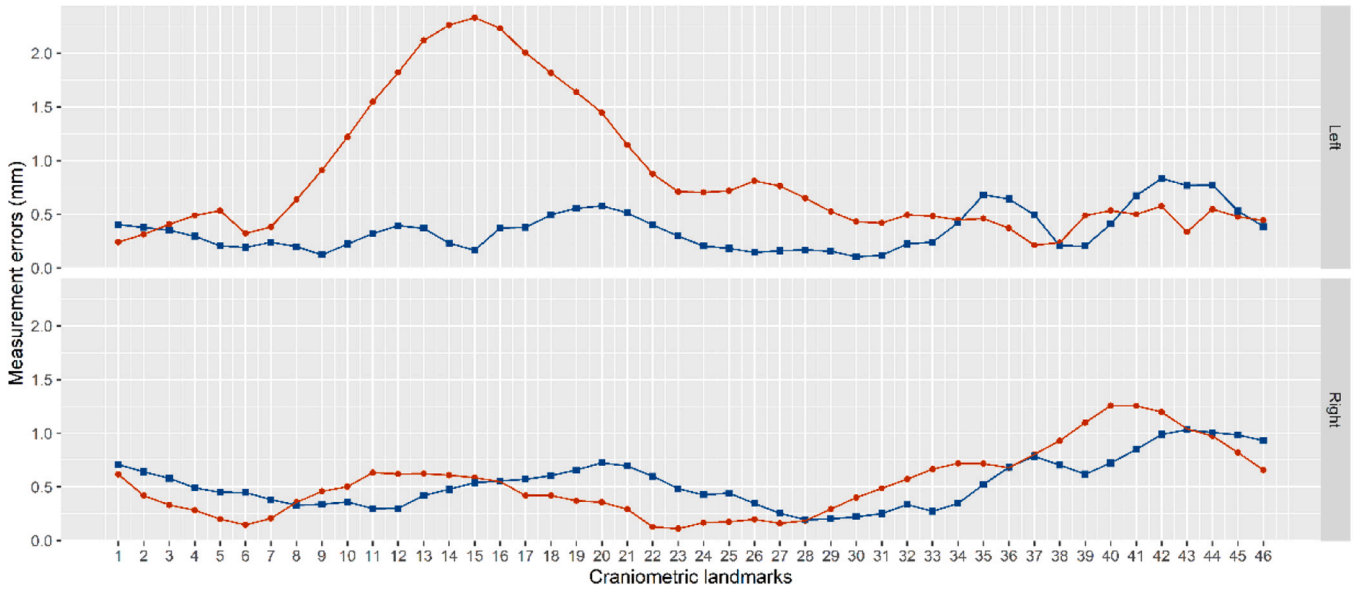

Fig. 3. Average dispersion for craniometric landmark placements (external auditory meatus). Red circle represents INTRA-OE. Blue square represents INTER-OE.

Results

Reproducibility testing

The overall average landmark measurement errors were < 2 mm for all four landmark configurations assessed (Table 2). Errors in the automatically placed landmarks would have been influenced by any incorrect manual placements on the template, which must be taken into consideration when interpreting results.

For the left ear, lobule posterior and supra-anguli conchali were the landmarks with the highest dispersion errors for placement between two observers (> 2 mm). For the intra-observer test, the landmarks superhelixa interna, superaurale, otobasion superius, preaurale, and supra-anguli conchali had the highest dispersion errors (> 2 mm). In the inter-observer test for the right ear the landmarks with the highest dispersion error (> 3 mm) are postaurale and supra-anguli conchali

Table 3
Results of the ANOVA test for significance of asymmetry between mean shapes of the left and right sides.

Structures assessed for asymmetry	Complete sample	Black South Africans	White South Africans
Ears	< 0.01 *	< 0.01 *	< 0.01 *
EAMs	< 0.01 *	< 0.01 *	< 0.01 *

EAM = external auditory meatus
*Indicates statistically significant results

Table 4
Significance of variation in mean ear and EAM shape population affinity (black and white South Africans).

	MANOVA *Population affinity*	50/50 MANOVA *Population affinity*	Permutation test *Population affinity*	ANOVA *Population affinity*Size*
Left ear	0.001 *	< 0.001 *	0.001 *	0.501
Right ear	0.001 *	< 0.001 *	0.001 *	0.501
Left EAM	0.001 *	< 0.001 *	0.001 *	0.503
Right EAM	0.001 *	< 0.001 *	0.001 *	0.112

EAM = external auditory meatus
*Indicates statistically significant results

(Fig. 2). For craniometric landmarks, the initial landmark porion was placed with a dispersion error of less than 1 mm. Overall, placements are more accurate between the same observer than between different observers, with all placements with an error of less than 1 mm for almost all landmarks in the INTER-OE test. Landmark displacement on the left EAM had the highest mean dispersion error (Fig. 3).

Preliminary results for normality

The distributions of Q-Q plots were visually assessed to ensure normality of the data. All landmark configurations displayed only minimal or slight deviation from normality. To ensure reliability of significant variables, results from both parametric and non-parametric tests were interpreted.

Shape analysis

Statistically significant variation exists between the shape of the left and right side of an individual for both the ears and the EAMs (Table 3). Therefore, all structures were analyzed as left and right separately in subsequent statistical testing. The influence of population affinity, sex, and age was assessed through parametric and non-parametric testing.

Population affinity was observed to significantly influence the shape of the ear and EAM for both left and right sides in all parametric and non-parametric tests performed (Table 4). However, when assessing the influence between population affinity and allometry on ear and EAM shape simultaneously, no results were statistically significant. Statistical separation of the top two PC scores between population affinity groups was less defined in the soft tissue configurations (Fig. 4) than the hard tissue configurations (Fig. 5). White South Africans present with a larger mean centroid size in the left ear, whereas black South Africans have a larger mean centroid size for the right ear. For the EAM, black South Africans present with a larger mean centroid size for the left side, and white South Africans with a slightly larger mean centroid size for the right side (Fig. 6).

The influence of sex on biological shape was assessed on both the complete sample, and on each population affinity subsample separately to account for the difference in sexual dimorphism between populations. Sex was found to be statistically significant on shape of the right ear and right EAM for the complete sample, and both ears and the right EAM for white South Africans (Table 5). Although males displayed more variation in shape than females, females presented with larger mean centroid sizes for both left and right ears and EAMs (Fig. 7). Sexual dimorphism in ear and EAM shape was assessed in co-variation with population affinity (Table 6), but none of the structures provided significant results for both parametric and non-parametric tests. The co-variation between sex and allometry was not significant for any of the matrices.

Age only significantly influenced shape for all tests in the left ear for white South Africans. None of the variables assessed significantly

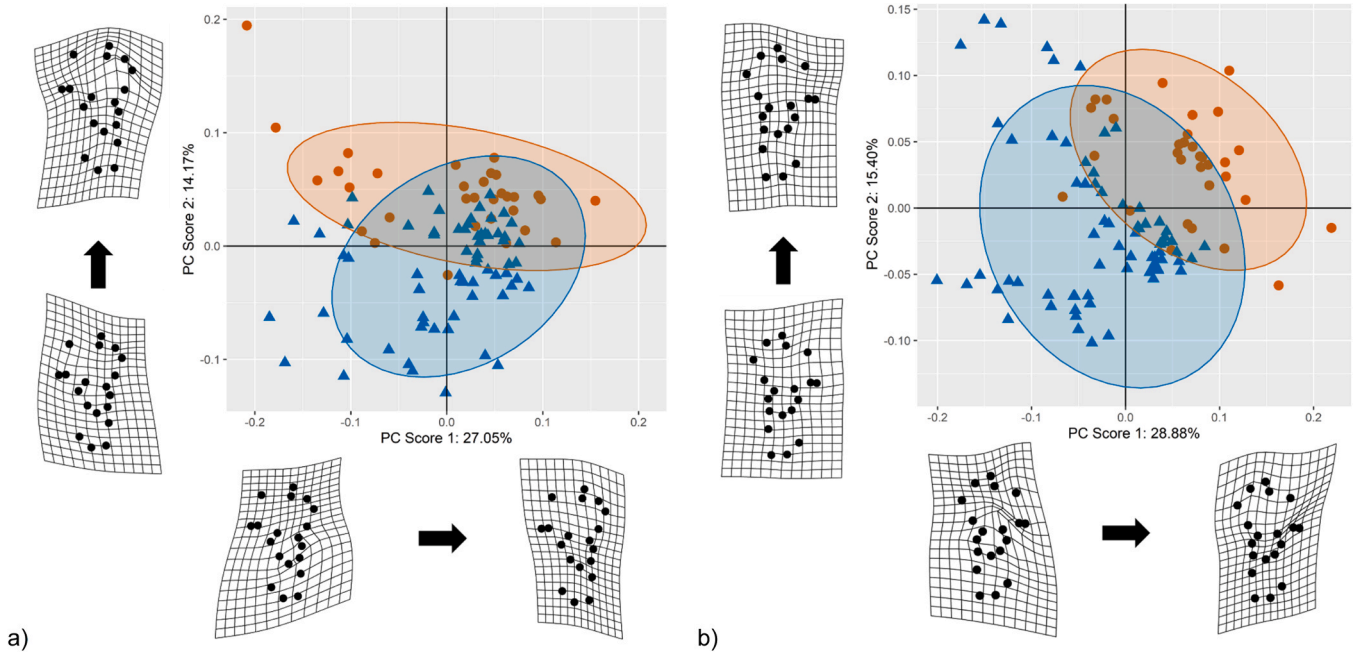

Fig. 4. Scatterplots for variance between population affinity and minimum and maximum shapes along PC scores 1 and 2 for soft tissue ears. Orange circles represents black South Africans. Blue triangles represents white South Africans. a) Left ear, b) Right ear.

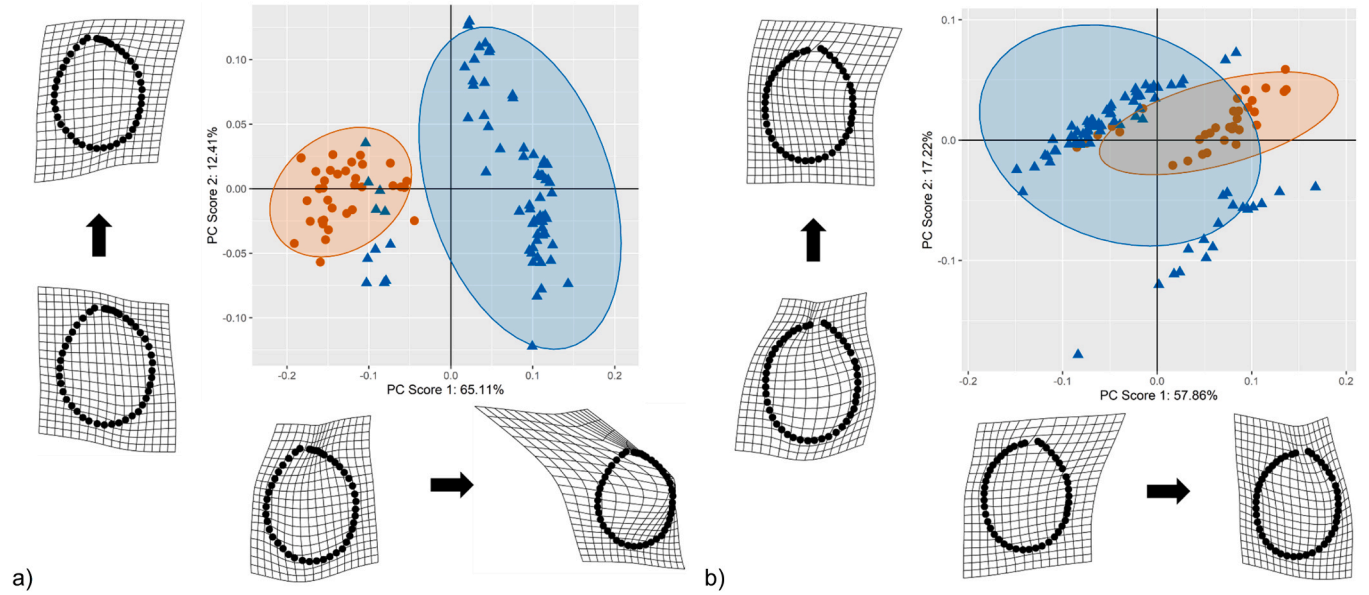

Fig. 5. Scatterplots for variance between population affinity and minimum and maximum shapes along PC scores 1 and 2 for hard tissue EAM. Orange circles represent black South Africans. Blue triangles represent white South Africans. a) Left EAM, b) Right EAM.

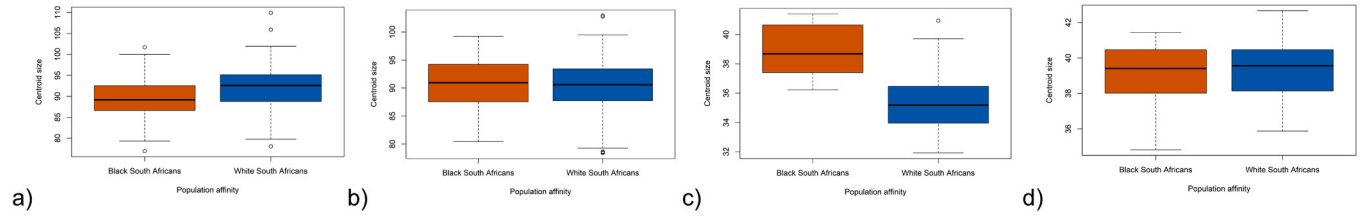

Fig. 6. Boxplots depicting centroid sizes of the shape components for comparison between population affinity. a) Left ear, b) Right ear, c) Left EAM, d) Right EAM.

Table 5
Significance of variation in mean ear and EAM shape between sexes (males and females).

	Complete sample			Black South Africans			White South Africans		
	MANOVA	50/50 MANOVA	Permutation test	MANOVA	50/50 MANOVA	Permutation test	MANOVA	50/50 MANOVA	Permutation test
Left ear	0.088	0.131	0.085	0.195	0.289	0.202	0.001 *	< 0.001 *	0.001 *
Right ear	0.001 *	< 0.001 *	0.001 *	0.356	0.486	0.361	0.001 *	< 0.001 *	0.001 *
Left EAM	0.935	0.818	0.925	0.414	0.515	0.432	0.668	0.714	0.679
Right EAM	0.030 *	0.001 *	0.060	0.456	0.211	0.454	0.007 *	< 0.001 *	0.006 *

EAM = external auditory meatus
*Indicates statistically significant results

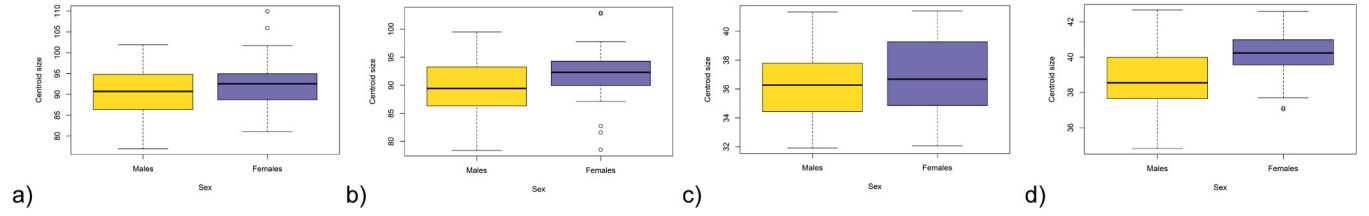

Fig. 7. Boxplots depicting centroid sizes of the shape components for comparison between sexes. a) Left ear, b) Right ear, c) Left EAM, d) Right EAM.

influenced the shape of the left or right ears and EAMs in the black South African sample (Table 7). Age was also not a significantly influencing factor when assessed in co-variation with population affinity or sex for either the left or right ear or EAM (Table 8). Centroid sizes visualised by boxplots revealed that the 60 + years cohort had higher means for the left and right ear, 45 – 59 years had the largest mean for the left EAM, and 30 – 44 years had the largest mean centroid size for the right EAM (Fig. 8).

Table 6
Significance of co-variation in mean ear and EAM shape between population affinity, sex, and allometry.

	Complete sample *Sex*Population affinity*		Complete sample *Sex*Size*	Black South Africans *Sex*Size*	White South Africans *Sex*Size*
	50/50 MANOVA	MANCOVA	ANOVA	ANOVA	ANOVA
Left ear	0.208	0.016 *	0.501	0.582	0.501
Right ear	< 0.001 *	0.138	0.501	0.563	0.501
Left EAM	< 0.001 *	0.725	0.503	0.560	0.544
Right EAM	< 0.001 *	0.002	0.112	0.571	0.501

EAM = external auditory meatus
*Indicates statistically significant results

The influence of shape on size could only be considered significant for the complete sample of left EAMs (Table 9), and had no significant influence on the soft tissue ears. Assessing co-variation of allometry with the variables population affinity or sex did not increase the statistical significance of size on shape for either ear or EAM.

A DFA was performed to assess classification accuracies for ear and EAM shape on the complete sample and on each population group separately (Table 10). Classifications for population affinity were the most reliable with accuracies above 80% for both ears and EAMs. Classifications accuracies for sex were lower (between 60% and 80%), and age resulted in the lowest classification accuracies – all below 50%.

Assessment of correlations between the ear and underlying EAM revealed strong positive correlations for both left and right sides (Table 11). All correlations were also statistically significant.

Discussion

Forensic Facial Approximations (FFA) used to identify unknown individuals is a long and detailed process but necessary in cases where fingerprints and DNA comparisons cannot be used – a common occurrence in the South African setting [42]. Automating the facial approximation process using computerized methods and 3D medical scanning technology allows for faster approximations and multiple representations of the individual [6,44]. The continuous development of computerized databases will aid in generating faster, easier, and more accurate facial approximations for unknown individuals by correlating selected cranial landmarks to soft tissue representations [6,21,44]. The results of this study support the need for population-specific databases for computerized 3D facial approximations, with an emphasis on estimating facial feature shape based on population-specific data. As the discipline of FFA shifts towards an automated and computerized 3D approach, large databanks of population-specific data must be created to create statistical models for predicting soft tissue facial features based on hard tissue structures. Ear shape has been commonly ignored in the literature and standard casts are used instead [2,43], but for an automatic facial approximation, an accurate estimate of the ear based on population affinity, sex, and age-specific guidelines is required.

Table 7
Significance of variation in mean ear and EAM shape between age cohorts.

	Complete sample		Black South Africans		White South Africans	
	MANOVA	50/50 MANOVA	MANOVA	50/50 MANOVA	MANOVA	50/50 MANOVA
Left ear	0.043 *	0.064	0.661	0.423	0.013 *	0.013 *
Right ear	0.444	0.381	0.377	0.409	0.133	0.132
Left EAM	0.279	0.473	0.126	0.077	0.057	0.111
Right EAM	0.769	0.658	0.102	0.098	0.835	0.869

EAM = external auditory meatus
*Indicates statistically significant results

Table 8
Significance of co-variation in mean ear and EAM shape between age, population affinity, and sex.

	Complete sample *Age*Population*		Complete sample *Age*Sex*		Complete sample *Age*Sex*Population*		Black South Africans *Age*Sex*		White South Africans *Age*Sex*	
	50/50 MANOVA	MANCOVA	50/50 MANOVA	MANCOVA	50/50 MANOVA	MANCOVA	50/50 MANOVA	MANCOVA	50/50 MANOVA	MANCOVA
Left ear	0.862	0.457	0.697	0.073	0.955	0.212	0.870	0.655	0.420	0.020 *
Right ear	0.057	0.551	0.801	0.799	0.163	0.606	0.397	0.755	0.178	0.120
Left EAM	< 0.001 *	0.312	0.397	0.184	< 0.001 *	0.406	0.298	0.250	0.444	0.254
Right EAM	< 0.001 *	0.665	0.754	0.607	0.011 *	0.154	0.289	0.512	0.859	0.057

EAM = external auditory meatus
*Indicates statistically significant results

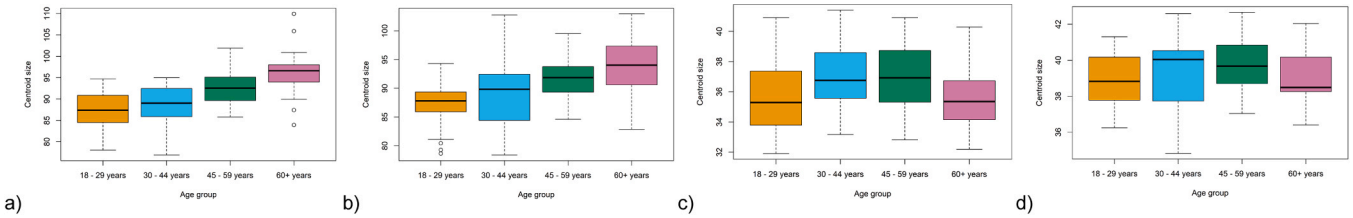

Fig. 8. Boxplots depicting centroid sizes of the shape components for comparison between age cohorts. a) Left ear, b) Right ear, c) Left EAM, d) Right EAM.

Table 9
Significance of co-variation in mean ear and EAM shape between allometry, population affinity and sex.

	Complete sample *Size*		Complete sample *Size*Population*		Complete sample *Size*Sex*		Complete sample *Size*Population*Sex*		Black South Africans *Size*Sex*		White South Africans *Size*Sex*	
	50/50 MANOVA	MANCOVA	50/50 MANOVA	MANCOVA	50/50 MANOVA	MANCOVA	50/50 MANOVA	MANCOVA	50/50 MANOVA	MANCOVA	50/50 MANOVA	MANCOVA
Left ear	0.838	0.146	0.782	0.695	0.620	0.384	0.988	0.577	0.960	0.910	0.673	0.513
Right ear	0.209	0.323	0.599	0.905	0.839	0.785	0.807	0.897	0.720	0.757	0.726	0.598
Left EAM	< 0.001 *	< 0.001 *	0.082	< 0.001 *	< 0.001 *	0.345	< 0.001 *	0.696	0.250	0.620	0.006 *	0.322
Right EAM	0.644	0.021 *	0.011 *	0.019 *	0.800	0.380	0.077	0.706	0.067	0.804	0.311	0.580

EAM = external auditory meatus
*Indicates statistically significant results

Table 10
Classification accuracies for population affinity, sex, and age through DFA.

	Population affinity	Sex			Age		
	Complete sample	Complete sample	Black South Africans	White South Africans	Complete sample	Black South Africans	White South Africans
Left ear	86%	65%	66%	80%	36%	47%	41%
Right ear	91%	71%	63%	73%	35%	35%	33%
Left EAM	89%	61%	63%	62%	31%	31%	43%
Right EAM	82%	69%	66%	62%	36%	36%	24%

EAM = external auditory meatus

Table 11
Partial Least Squares correlations between the soft tissue ear and underlying EAM for left and right sides.

	Complete sample		Black South Africans		White South Africans	
	r^2-PLS	p-value	r^2-PLS	p-value	R^2-PLS	p-value
Left EAM†	0.839	0.001 *	0.792	0.001 *	0.871	0.001 *
Right EAM‡	0.844	0.001 *	0.860	0.001 *	0.877	0.001 *

EAM = external auditory meatus
*Indicates statistical significance
† Correlated to left ear
‡ Correlated to right ear

The left and right sides were assessed individually after statistically significant variation was observed between the left and right ears and EAMs, which differs from previous studies that found general bilateral symmetry in an individual's left and right ear [20,44]. GMM analysis could further identify significant variations in shape between population groups, sexes, and age cohorts. Population affinity contributed the most to variation in shape for both the ears and EAMs – most likely attributable to broad ecogeographical factors influencing the shape of soft-tissue features based on different climates of origin for those of African and European descent [10,11,13].

Overall, the influence of sex and age is less important on shape of the ears and EAMs; differing from literature assessing variation in ear size between sex and age cohorts where significant variations are observed. In the existing literature, males are consistently found to have larger ears than females, but the influence of size on ear shape does not significantly differ between sexes in this study. In a French sample, 9% of variation in ear shape between males and females could be attributed to size [21], whereas in the current study the co-variation of allometry and sex had no effect. Age is also cited to significantly influence ear size as the ear undergoes continuous lengthening throughout life [16,19,20], whereas this study revealed inconsistent results for the significant influence of age on ear shape. Assessing covariation between sex and age did not reveal a significant influence on shape, but once population affinity was included as a covariate for assessment, structures had a higher rate of significant influence – albeit inconsistent across tests run. The importance of the influence of population affinity is again supported by the much higher classification accuracy derived from DFA when comparing population groups, compared to lower rates of significance when assessing the influence of sex and age through shape. Sample sizes must be considered when interpreting these results, possibly masking existing variation due to an unequal number of individuals in each category. For example, the insignificant influences of sex, age, and allometry on shape for the black South African sample could result from a smaller cohort sizes than the white South Africans. Knowing that population affinity is the most significant influence on the shape of the soft tissue ear supports the need for population-specific databanks for automatic facial approximations. However, the effects of sex, allometry, and age on shape could likely only become statistically significant when all subsamples are substantially increased, or size such as ear height and breadth is further investigated.

Conclusion

No two ears are indeed the same, not even for the same individual's left and right sides. While an ear will never be exactly recreated, basing estimates on the individual's biological profile can lead towards the highest accuracies possible for approximations. This research is the first assessment of ear shape in a South African sample. By using CBCT databases, both the hard and soft tissue structures were assessed for the same individual – allowing for accurate correlations between surfaces of an individual, and between population groups. Employing 3D techniques also allowed for comprehensive analysis of the hard and soft tissues between both individuals and larger samples, as well as detailed analysis of shape variation – specifically for the curvature of the EAM. By assessing the influences of population affinity, sex, and age on ear shape, this research can aid in the development of guidelines for approximations of the ear specific to an individual and contribute to improving facial approximation methods used in South Africa. The influence of

broad geographical ancestry is evident in the influence of the soft tissue ear and underlying hard tissues and supports the need for population specific databases. Regarding shape – specifically for the ear – sex and age will not be a priority when creating approximation methods and mean shapes based on the individual's population affinity only can be modelled. Still, based on previous literature, size will likely be an important factor to consider when estimating the ear of an individual based on their sex and age. Therefore, size should be further investigated on a South African sample and incorporated into shape analyses to develop comprehensive ear estimates.

Funding

This project has been funded with support from the European Commission through the Bakeng se Afrika project (Grant number 597924-EPP-2018–1-ZA-EPPKA2-CBHE-JP). This publication reflects the views only of the author, and the Commission cannot be held responsible for any use which may be made of the information contained therein.

Declaration of Competing Interest

The authors declare no conflict of interest in the preparation of this research and the submitted manuscript.

Acknowledgements

The authors would like to thank Dr André Uys from the Oral and Dental Hospital, University of Pretoria, and Dr Sarel Botha from the Groenkloof Life Hospital, Pretoria, South Africa, for the initial scan acquisition and allowing access to the CBCT databases. The authors would also like to thank the University of Pretoria Postgraduate Bursary Scheme for supporting this research.

References

[1] M.M. Gerasimov, Vosstanovlenie lica po cerepu, Akad. Nauk SSSR, Mosk., Izdat (1955).
[2] C. Wilkinson, Facial reconstruction - anatomical art or artistic anatomy, J. Anat. 216 (2010) 235–250.
[3] P. Guyomarc'h, C.N. Stephan, The validity of ear prediction guidelines used in facial approximation, J. Forensic Sci. 57 (2012) 1427–1441, https://doi.org/10.1111/j.1556-4029.2012.02181.x.
[4] H. Ullrich, C.N. Stephan, On gerasimov's plastic facial reconstruction technique: new insights to facilitate repeatability, J. Forensic Sci. 56 (2011) 470–474, https://doi.org/10.1111/j.1556-4029.2010.01672.x.
[5] W. Lee, C. Wilkinson, H. Hwang, An accuracy assessment of forensic computerized facial reconstruction employing cone-beam computed tomography from live subjects, J. Forensic Sci. 57 (2012) 318–326, https://doi.org/10.1111/j.1556-4029.2011.01971.x.
[6] D. Vandermeulen, P. Claes, D. Loeckx, S. De Greef, G. Willems, P. Suetens, Computerized craniofacial reconstruction using CT-derived implicit surface representations, Forensic Sci. Int. 159S (2006) S164–S174.
[7] A.F. Ridel, F. Demeter, M. Galland, E.N. L'Abbé, D. Vandermeulen, A.C. Oettlé, Automatic landmarking as a convenient prerequisite for geometric morphometrics. Validation on cone beam computed tomography (CBCT)- based shape analysis of the nasal complex, Forensic Sci. Int. 306 (2020), https://doi.org/10.1016/j.forsciint.2019.110095.
[8] L. Verzé, History of facial reconstruction, Acta Biomed. 80 (2009) 5–12.
[9] T.D. White, A. Ortega-Castrillón, H. Matthews, A.A. Zaidi, O. Ekrami, J. Snyders, P. Claes, MeshMonk: Open-source large-scale intensie 3D phenotyping, Nat. Sci. Rep. 9 (2019), https://doi.org/10.1038/s41598-019-42533-y.
[10] N.J. Sauer, Forensic anthropology and the concept of race: if races don't exist, why are forensic anthropologists so good at identifying them? Soc. Sci. Med. 34 (1992) 107–111.
[11] S. Ousley, R. Jantz, D. Fried, Understanding race and human variation: why forensic anthropologists are good at identifying race, Am. J. Phys. Anthropol. 139 (2009) 68–76, https://doi.org/10.1002/ajpa.21006.
[12] H.F. Smith, C.E. Terhune, C.A. Lockwood, Genetic, geographic, and environmental correlates of human temporal bone variation, Am. J. Phys. Anthropol. 134 (2007) 312–322, https://doi.org/10.1002/ajpa.20671.
[13] K.E. Stull, M.W. Kenyhercz, E.N. L'Abbé, Ancestry estimation in South Africa using craniometrics and geometric morphometrics, Forensic Sci. Int. 245 (2014) 206.e1–206.e7, https://doi.org/10.1016/j.forsciint.2014.10.021.
[14] K.S. Alexander, D.J. Scott, B. Sivakumar, N. Kang, A morphometric study of the human ear, J. Plast., Reconstr. Aesthetic Surg. 64 (2010) 41–47.
[15] L. Meijerman, C. van der Lugt, G.J.R. Maat, Cross-sectional anthropometric study of the external ear, J. Forensic Sci. 52 (2007) 268–293, https://doi.org/10.1111/j.1556-4029.2006.00376.x.
[16] C. Sforza, G. Grandi, M. Binelli, D.G. Tommasi, R. Rosati, V.F. Ferrario, Age- and sex-related changes in the normal human ear, Forensic Sci. Int. 187 (2009) 110.e1–110.e7.
[17] W. Lee, X. Yang, H. Jung, I. Bok, C. Kim, O. Kwon, H. You, Anthropometric analysis of 3D ear scans of Koreans and Caucasians for ear product design, Ergonomics 61 (2018) 1480–1495.
[18] E.A. Osunwoke, W.B. Vidona, G.C. Atulegwu, Anthropometric study on the anatomical variation of the external ear amongst Port Harcourt students, Nigeria, Int. J. Anat. Var. 11 (2018) 143–146.
[19] R. Purkait, P. Singh, Anthropometry of the normal human auricle: a study of adult Indian men, Aesthetic Plast. Surg. 31 (2007) 372–379, https://doi.org/10.1007/s00266-006.0231.4.
[20] R. Purkait, External ear: an analysis of its uniqueness, Egypt. J. Forensic Sci. 6 (2016) 99–107.
[21] P. Guyomarc'h, B. Dutailly, J. Charton, F. Santos, P. Desbarats, H. Coquegniot, Anthropological Facial Approximation in Three Dimensions (AFA3D): Computer-assisted estimation of the facial morphology using Geometric Morphometrics, J. Forensic Sci. 59 (2014) 1502–1516, https://doi.org/10.1111/1556-4029.12547.
[22] U. Ozsoy, R. Sekerci, E. Ogut, Effect of sitting, standing, and supine body positions on facial soft tissue: Detailed 3D analysis, Int. J. Oral. Maxillofac. Surg. 44 (2015), https://doi.org/10.1016/j.ijom.2015.06.005.
[23] L. Munn, C.N. Stephan, Changes in face topography from supine-to-upright position - And soft tissue correction values for craniofacial identification, Forensic Sci. Int. 289 (2018) 40–50, https://doi.org/10.1016/j.forsciint.2018.05.016.
[24] H. Chen, M. van Eijnatten, G. Aarab, T. Forouzanfair, J. de Lange, P. van der Stelt, F. Lobbezoo, J. Wolff, Accuracy of MDCT and CBCT in three-dimensional evaluation of the oropharynx morphology, Eur. J. Orthod. (2018) 58–64, https://doi.org/10.1093/ejo/cjx030.
[25] A.F. Ridel, J. Liebenberg, E.N. L'Abbé, D. Vandermeulen, A.C. Oettlé, Skeletal dimensions as predictors for the shape of the nose in a South African sample: a cone-beam computed tomography (CBCT) study, Forensic Sci. Int. 289 (2018) 18–26, https://doi.org/10.1016/j.forsciint.2018.05.011.
[26] F. Bookstein, Morphometric Tools for Landmark Data: Geometry and Biology, Cambridge University Press, Cambridge, England, 1991.
[27] D.E. Slice, Geometric morphometrics, Annu. Rev. Anthropol. 36 (2007) 261–281.
[28] P. Mitteroecker, P. Gunz, Advances in geometric morhpmetrics, Evolut. Biol. 36 (2009) 235–247.
[29] C.F. Spoor, F.W. Zonneveld, G.A. Macho, Linear measurements of cortical bone and dental enamel by computed tomography: applications and problems, Am. J. Phys. Anthropol. 91 (1993) 469–484.
[30] J.M. Caple, C.N. Stephan, A standard nomenclature for craniofacial and facial anthropometry, Int. J. Leg. Med. 130 (2016) 863–879.
[31] A. Ridel, F. Demeter, M. Galland, E. L'abbé, D. Vandermeulen, A. Oettlé, Automatic landmarking as a convenient prerequisite for geometric morphometrics. Validation on cone beam computed tomography (CBCT)- based shape analysis of the nasal complex, Forensic Sci. Int. 306 (2020), 110095, https://doi.org/10.1016/j.forsciint.2019.110095.
[32] G. Ocakoğlu, S. Turan Özdemİr, İ. Ercan, A. Etöz, The shape of the external human ear: a geometric morphometric study, Turk. Klin. J. Med. Sci. 33 (2013) 184–190.
[33] D.G. Kendall, Shape manifolds, procrustean metrics, and complex projective spaces, Bull. Lond. Math. Soc. 16 (1984) 81–121.
[34] I.L. Dryden, K.V. Mardia, Statistical shape analysis: with applications in R, John Wiley & Sons, 2016.
[35] L. Scrucca, Assessing multivariate normality through interactive dynamic graphics, Quad. Di Stat. 2 (2000) 221–240.
[36] S. Schlager, Morpho: Calc. Vis. Relat. Geom. Morphometrics (2017).
[37] C.P. Klingenberg, M. Barluenga, A. Meyer, Shape analysis of symmetric structures: quantifying variation among individuals and asymmetry, Evolution 56 (2002) 1909–1920.
[38] D.C. Adams, M. Collyer, A. Kaliontzopoulou, Geom. morphometric Anal. 2D/3D Landmark data (2018).
[39] Ø. Langsrud, 50-50 multivariate analysis of variance for collinear responses, J. R. Stat. Soc. 51 (2002) 305–347.
[40] Ø. Langsrud, B.H. Mevik, Fifty-fifty MANOVA, (2012). http://CRAN. R-project.org/package= ffmanova.
[41] P. Mitteroecker, P. Gunz, S. Windhager, K. Schaefer, A brief review of shape, form, and allometry in geometric morphometrics, with applications to human facial morphology, Hystrix, Ital. J. Mammal. 24 (2013) 59–66, https://doi.org/10.4404/hystrix-24.1-6369.
[42] M.Y. İşcan, M. Steyn, Facial approximation and skull-photo superimposition. in: The Human Skeleton in Forensic Medicine, Charles C. Thomas Publishing Ltd,, Springfield, Illinois, 2013, pp. 361–392.
[43] H. Ullrich, C.N. Stephan, Mikhail Mikhaylovich Gerasimov's authentic approach to basic facial reconstruction, Anthr. LIV 2 (2016) 97–107.
[44] P. Claes, J. Reijniers, M.D. Shriver, J. Snyders, P. Suetens, J. Nielandt, G. De Tré, D. Vandermeulen, An investigation of matching symmetry in the human pinnae with possible implications for 3D ear recognition and sound localisation, J. Anat. 226 (2015) 60–72.